ResearchGate

See discussions, stats, and author profiles for this publication at: https://www.researchgate.net/publication/313249361

Influences of Energy Throughput on the Life of Various Battery Technologies

Conference Paper · October 2016

CITATIONS
0

READS
88

2 authors:

Brian De Beer
Stellenbosch University
2 PUBLICATIONS **0** CITATIONS
SEE PROFILE

Arnold Rix
Stellenbosch University
23 PUBLICATIONS **81** CITATIONS
SEE PROFILE

All content following this page was uploaded by Arnold Rix on 03 February 2017.

The user has requested enhancement of the downloaded file.

Influences of Energy Throughput on the Life of Various Battery Technologies

Brian de Beer[1], **Arnold J. Rix**[2]

Department of Electrical and Electronic Engineering, Stellenbosch University, Cnr of Banghoek Rd and Joubert St, 7600, Stellenbosch, South Africa

E-Mail: [1]16945484@sun.ac.za, [2] rix@sun.ac.za

Abstract

The growing integration of solar photovoltaic systems into the national power grid has the potential to increase grid instability. Instability is caused by the fluctuating irradiance on the solar panels owing to weather conditions such as passing cloud cover. These fluctuations can be mitigated by energy storage systems such as batteries. Selecting the correct battery technology is a challenge since affordability and performance are important deciding factors. A method is required to determine which battery technology will be the superior option while also satisfying all the design criteria, in other words, a method which estimates the life span of different battery technologies based on operational conditions determined by the user (in this case, the regional weather).

A battery state-of-health model and a fluctuation mitigation model are identified and selected. The models are tested separately and then combined to create a final model. The results produced indicate that the fluctuation mitigation utilises the batteries in such a way that battery life is optimised and that the battery capacity and depth-of-discharge will determine the mitigation performance.

It is found that the two models work well together. The model methods can be questioned and have yet to be tested practically.

1. Introduction

A growing solar industry can be observed in South Africa. This is due to the affordability of solar technology paired with the availability of irradiance. It is observed on a residential as well as a utility scale. The production of solar energy has a lot of advantages such as cleaner energy production and more available energy in a country where the supply infrastructure cannot always meet the demand. However, there are some concerns regarding the growth of this industry.

The increased integration of solar power generating systems into the grid causes instability owing to the fluctuations in solar irradiance. The national electrical utility (ESKOM) may struggle to mitigate these fluctuations in the future. On the solar energy provider's side, one method to address this issue is to apply an energy storage solution

Controlling and monitoring the battery systems and inverters, as shown in Figure 1, will be the focus for the models. These systems have the ability to deliver or absorb certain amounts of energy depending on the size. The size of the battery system is directly proportionate to its cost. Since batteries are an expensive part of renewable energy systems, it is important to determine the minimum required size to fit the design specifications. An example is the backup energy systems found residential homes. The energy throughput of these systems plays an important role in the lifetime of the batteries. It is thus important to match certain battery technologies to certain energy throughputs or usage schemes. These are determined by regional weather patterns and thereby minimize the system cost by maximising system battery lifetime to mitigate the fluctuations on the photovoltaic (PV) output.

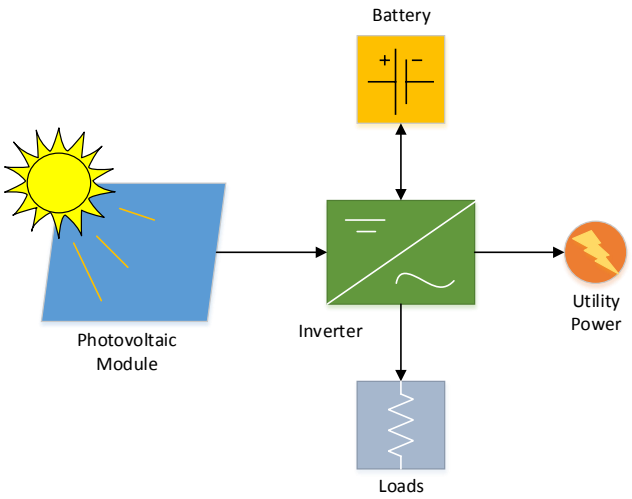

Fig. 1. Photovoltaic energy system.

Matching battery systems to certain usage schemes requires energy throughput profiles. These profiles can be

determined by implementing a smoothing algorithm which determines when energy should be delivered or absorbed and how much. A model is required to compare the different energy profiles to different battery technologies. In order to achieve this, a battery state-of-health (SOH) model will be used to draw a comparison. The SOH model will use the energy throughput profiles as inputs to compare various systems of different sizes from regional weather data in order to determine which battery technology fits the profile best.

2. Batteries

Different battery technologies exist and each has their own advantages and disadvantages. This project will include the two main battery technologies which are currently being considered in projects. The two presented batteries are lead-acid (Pb-SO) and lithium-ion(Li-ion). These are discussed below:

1) Li-ion: Lithium-ion batteries have a positive electrode (e.g. aluminium with an active material such as lithium cobalt oxide) and negative electrode (e.g. copper with a carbonaceous material such as graphite) between which ions move to produce a flowing current [1].

These batteries are known to have high efficiencies. The advantages of Li-ion batteries include high energy-to-weight ratios, low self-discharge, no memory effect and a specific energy of about 200 W·h/kg which is five times that of lead acid batteries [2]. Disadvantages include the use of safety circuits which act as battery management systems to allow for special charging methods. These safety circuit make the batteries more expensive. Another disadvantage of the Li-ion batteries is how expensive the technology is relative to that of some of its competitors. This high price may continue to be a problem due to the limited resources and the further depletion due to an increased use in electric vehicles (EV) and hybrid electric vehicles (HEV) [3, 4].

Lithium-ion batteries are mainly used in portable devices such as cameras, mobile phones, portable tools and laptops. In recent years, these batteries are also widely used in EV and HEV applications.

2) $PbSO_4$: The lead-acid battery is one of the most common and well-known types of batteries in industry. This type of battery consists of a positive and negative electrode with lead dioxide and spongy lead as active materials, respectively. Diluted sulphuric acid is used as the electrolyte. [2]

Advantages of Pb-acid batteries include the ability to be resistant to abuse, and low cost compared to competing battery types. Disadvantages include the low energy density per kilogram, slower charging times, water loss during overcharge which leads to increased maintenance and limited cycle life. [2]

Pb-acid batteries are used in smaller residential scale PV systems, vehicle ignitions, uninterrupted power supply (UPS) systems and lighting.

Li-ion and lead-acid batteries are commonly discussed technologies and therefore these batteries will be compared using the method to be explained.

3. State-of-Health Models

In order to determine the usability of a battery, it is important to know the condition of that battery. To track the condition of the battery, a model is used. During this research into battery health estimation practices and the models used in these practices. These methods were compared and primarily consisted of electrochemical-, equivalent circuit- and energy-throughput models.

3.1. Electrochemical Models

The electrochemical models primarily focus on the details around the charge and discharge of chemical reactions and the chemical concentrations [5]. This model implements more technical algorithms than its counterparts. These models are considered very accurate but rely on a detailed set of specifications and parameters from manufacturers in order to be executed, which makes them complex and difficult to configure. These require a lot of time for testing, experimentation and data collection which only makes the results relevant to a specific battery. The limitations with regards to time and the relevance of the data makes this model inappropriate for use in this project.

3.2. Equivalent Circuit Model

The equivalent circuit model uses an electrical circuit, usually consisting of capacitors and resistors, that represents the characteristics of the battery. This model is also fairly accurate and can represent certain battery types as a whole. It relies on extensive testing and experimentation with the batteries in order to obtain the required characteristic variables [6]. These characteristic variables are used in equations to model how a battery reacts under certain conditions. This method is simpler than that of electrochemical models.

3.3. Ah-Throughput Model

In the Amp-hour-throughput model it is assumed that there is a fixed amount of energy throughput that a battery can handle before it is declared unusable due to capacity loss, regardless of the way the energy has been drawn [7]. This model uses simpler, pre-determined equations

which use data that is more readily available. This model is usually based on the depth-of-discharge (DoD) data which can be obtained from the manufacturer. This model is chosen for the present research since it is simple and provides relevant results for further use.

4. Ah-Throughput Model

The energy-throughput model is chosen for its simplicity and adaptiveness to form a more complex and accurate model to suit the present project's needs. The Ah-throughput model's expected throughput is based on the following equation [7]:

$$Ah_{tot} = \sum_{i=1}^{n} \frac{(E_{Nom} \cdot DoD_i) \cdot C_F}{n},$$

where E_{Nom} and DoD_i are the nominal battery capacity and depth of discharge, respectively. C_F is the number of cycles to failure for the specific DoD.

An energy throughput based capacity fade model, based on a modified Arrhenius equation, serves as the final selected model. This model is based on the assumption that DoD does not have a significant effect on the state-of-health (SOH) of the battery but rather that the rate at which energy is drawn and the operating temperatures of the battery play a critical role in the effect of health [8]. A C-rate of one is defined as the rate (in Ampere) at which a battery will be discharged in one hour. This enables the model to test how the different weather conditions affect the discharge patterns as well as battery temperatures. The equation to be implemented is as follows:

$$x(t) = x_0 - \frac{1}{2 \cdot N \cdot Ah_0(0)} \cdot \int_0^t |A_i(\tau)|\, d\tau, \qquad (1)$$

where $x_{2,0}$ and $Ah_0(0)$ are the initial state-of-health and initial Ah-capacity of the battery, respectively. N refers to the total number of cycles before end-of-life and A_i refers to the Ampere current in or out of the battery. The t indicates time. N can be calculated by the following modified Arrhenius equation [9]:

$$\Delta Ah_0 = B(c) \cdot exp\left(\frac{-E_a(c)}{R \cdot T}\right) \cdot A(c)^z, \qquad (2)$$

where ΔAh_0 refers to the allowable percentage capacity loss of the battery. $B(c)$ is the pre-exponential factor, $E_a(c)$ is the activation energy, c is the C-rate, R is the ideal gas constant, T is the lumped cell temperature and z is the power law factor which is fixed at 0.57 for the study [9]. $A(c)$ is the total Ah-throughout as a function of the C-rate which replaces time since it is directly proportionate to it[9]. Rearranging the formula, the following is obtained:

$$A(c) = \left[\frac{\Delta Ah_0}{B(c) \cdot exp\left(\frac{-E_a(c)}{R \cdot T}\right)}\right]^{1/z}, \qquad (3)$$

then we find N in equation 1 from:

$$N(c) = \frac{A(c)}{Ah_{cell}}. \qquad (4)$$

The model is implemented on Lithium-ion ($LiFePO_4$) batteries [10]. This battery will serve to represent Lithium-ion batteries as a whole. The lead-acid ($PbSO_4$) batteries are implemented using the original Arrhenius equation (equation 5) which is also adjusted to use Ah instead of time and, for this study, the focus will be on valve-regulated lead-acid (VRLA) batteries.

$$\Delta Ah_0 = B \cdot exp\left(\frac{-E_a}{R \cdot T}\right) \cdot A(c) \qquad (5)$$

The activation energy and pre-exponential factors of these batteries are indicated in Table 1 and 2. [10, 11]

	$E_a[J \cdot (mol \cdot K)^{-1}]$	B	Ah_{cell}
$LiFePO_4$	$31700 - 370,3 \cdot C$	Table 2	2.2
Lead-acid	71170	$^*2115 \times 10^7$	1.2

Table 1: Battery activation energies and pre-exponential factors [10, 11]

*The value was calculated using the original Arrhenius equation and the approximate amount of full charge/discharge cycles the battery technology can do in order to fit the model to the data in practical testing.

C-rate	$B(c)$
C/2	31630
2C	21681
6C	12934
10C	15512

Table 2: $LiFePO_4$ pre-exponential factors for certain C-rates [10]

4.1. Throughput Model Results

The throughput model is tested by selecting a battery system size (in this case 1000 Ah) based on the manufacturer's 5 hr rating. This rating is the closest to 1 C rating which is widely available. The tests are done at different C-rates and different temperatures for the two battery technologies. This is done to compare the model results

to available practical battery test results. The lead-acid model is set to 25 °C (298 K) at a 1 C-rating. The Li-ion model is set to 60 °C (333 K) at a 0.5 C-rating. The allowable battery capacity fade is set to 20 % which is widely used in the EV and HEV industry [8]. This means that the batteries are allowed to degrade to the point where 20 % of their capacity is lost before being declared unfit. Since the model is based on the Ah-throughput method, the results will be linear. This can be observed in the differences between the results in Figures 2 and 3 where the model is lower between the 100 % and 90 % capacity mark, on par at the 80 % mark and is higher between the 70 % and 60 % mark. The Li-ion battery results, shown in Figure 4, are similar to the practical results in Figure 5. The results appear nearly exact for each DoD.

5. PV Output Smoothing Models

PV fluctuations occur due to the variability of solar irradiance caused by passing cloud cover [12]. The effects are worse in a weaker distribution grid, causing significant voltage fluctuations. To mitigate this problem, the PV output needs to be conditioned. During this research, smoothing methods were investigated.

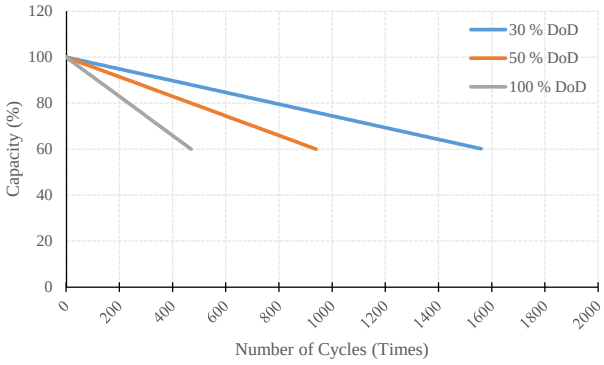

Fig. 2. Lead-acid battery model capacity degradation.

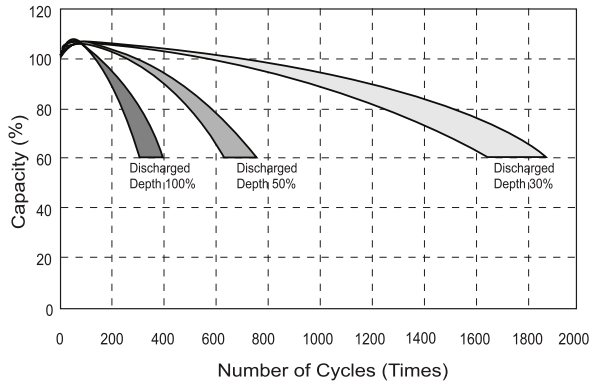

Fig. 3. Actual lead-acid battery capacity degradation. [13]

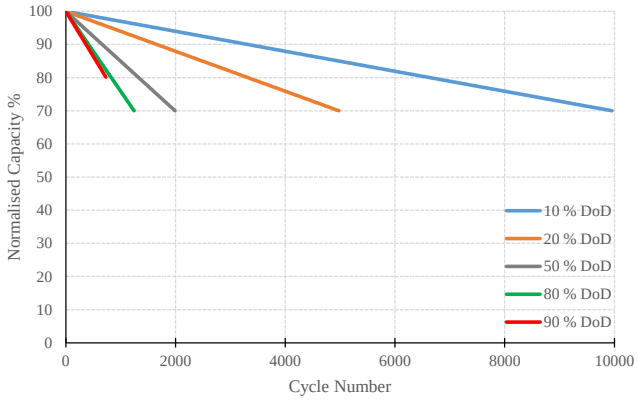

Fig. 4. Li-ion battery model capacity degradation.

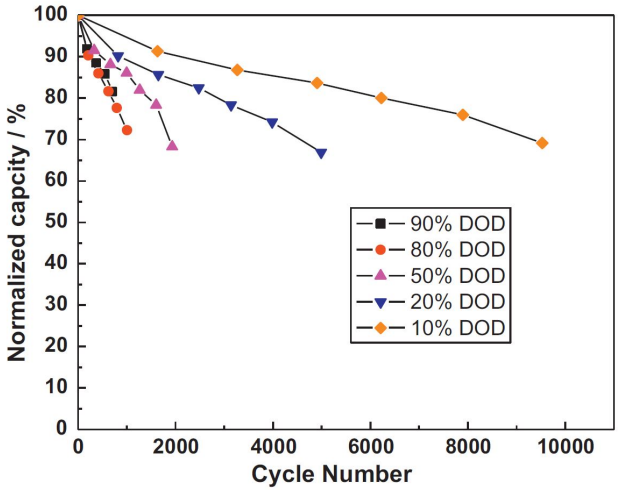

Fig. 5. Actual Li-ion battery capacity degradation. [10]

5.1. Moving Average Approach

This approach filters out fluctuations based on previous values. The method is essentially an average of a fixed amount of data points which are ever-changing as new data points are introduced. This method is the traditionally accepted smoothing method. The moving average method largely depends on the past history which could lead to its value differing significantly from the present value. This constant difference from the present causes the energy storage system to be utilised when it is not required and can be examined in Figure 6 (b). This method can also lack the desired ramp-rate depending on the length of the moving average.

5.2. Ramp-Rate Approach

This approach refers to the rate with which power increases or decreases. The power increases and decreases at the same rate as the irradiance levels. These irradiance levels are tied to the weather conditions at that moment. This

model keeps the ramp-rate within pre-determined limits, meaning it will track the solar PV output until there is an irradiance increase or decrease that exceeds the limits. In Figure 6 (a), the inverter output tracks the PV output till a sudden drop or increase occurs. At that moment the inverter will decrease or increase its power at a much slower ramp-rate, allowing the sudden fluctuations to be smoothed out. The drawing or absorbing of power is done with the help of the batteries. This method allows the battery system to be utilised only when necessary as indicated in Figure 6 (c).

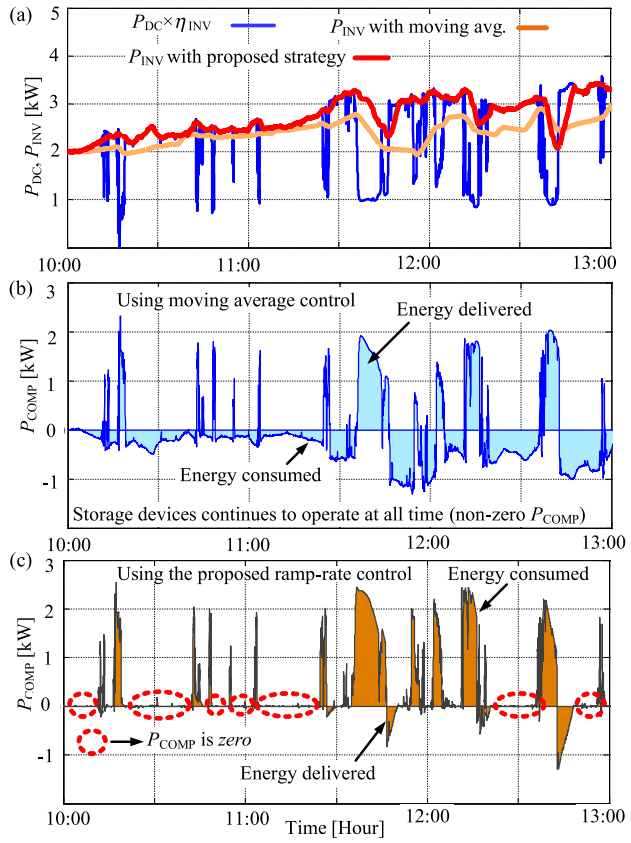

Fig. 6. PV fluctuation mitigation examples. (a) Profiles for P_{DC} and P_{INV}. (b) P_{COMP} for moving average. (c) P_{COMP} for ramp-rate control. [12]

6. Ramp-Rate Model

The ramp-rate model is chosen because it utilises batteries more effectively than the moving average method, thereby extending battery life and ensuring an economic operation of the system. This model is derived from the ramp-rate model in [12]. The mentioned model is adjusted since it has limitations with regards to post-ramping and could not adjust the ramp-rates as required. The ramp-rate model starts by calculating the PV ramp-rate (PVRR) from the PV output (P_{PV}). It is then determined whether or not the PVRR exceeds the ramp-rate limit. If the PVRR exceeds the ramp-rate limit, a new maximum allowable ramp-rate (MARR) is calculated as follows [12]:

$$MARR(k) = \begin{cases} |PVRR(k)|, & \text{if } |PVRR(k)| < RR_{lim} \\ \dfrac{\gamma}{PVRR(k)}, & \text{if } |PVRR(k)| \geq RR_{lim}, \end{cases} \tag{6}$$

where γ is the factor which controls the degree of dampening during a ramping event. This is known as the inverse characteristic constant. The ramp-rate limit (RR_{lim}) determines when the inverse characteristic will be applied. When the ramping event is within the limit, the system will just track the P_{PV} and apply the inverse characteristic only when the ramp-rate is exceeded. This is called the inverse characteristic-based desired ramp-rate strategy.

As shown in Figure 7, the MARR is compared to the PVRR and if it is found to be smaller, S is set equal to 1. S is a variable used to determine whether a compensating ramp-rate (RR_{COMP}) should be calculated or rather set to zero. The compensating ramp-rate is determined using the following [12]:

$$\frac{dP_{COMP}}{dt}(k) = S \times \left[\frac{1}{\eta_{inv}} \times \left\{MARR_{des} - \eta_{inv} \times f(\frac{dP_{DC}}{dt})\right\}\right], \tag{7}$$

where n_{inv} refers to the inverter efficiency, which can be obtained from the curve on the manufacturer's specification sheet, $MARR_{des}$ is the desired maximum allowed ramp rate and dP_{DC}/dt is a DC power ramp-rate.

If the PVRR is found to be smaller than MARR, it is required to check whether the previous power compensation ($P_{COMP}(k-1)$) was smaller than MARR. If it is found to be smaller, S is set equal to 0 and will result in zero compensation ramp-rate and $P_{COMP}(k)$. If $P_{COMP}(k-1)$ is found to be larger than MARR, the $P_{COMP}(k)$ needs to be calculated such that the system is tracking the output correctly. Calculating $P_{COMP}(k)$ requires RR_{COMP} and RR_{COMP}, and can be determined by examining whether the current power output (P_{OUT} of the system is larger or smaller than the actual P_{PV}. The result will indicate different input constants for calculating RR_{COMP} and can be summarised as in Table 3. The input parameters for RR_{COMP} are with reference to equation 7.

The compensating power can be calculated when RR_{COMP} has been determined. P_{COMP} can be calculated as follows [12]:

$$P_{COMP}(k) = S\times \left[P_{COMP}(k-1) + RR_{COMP}(k) \times \{t(k) - t(k-1)\}\right], \tag{8}$$

where $P_{COMP}(k-1)$ is the previous power compensation value and t refers to the time. Once the power compensation is calculated, a check is done to ensure whether the

charge or discharge of the batteries is within the set state-of-charge (SOC) limits and not exceeding the C-rate of 10. The C-rate limit of 10 is chosen since the model does not support accurate characteristic estimation beyond it. This ensures that the model can be applied to various battery sizes while only influencing the degree of smoothing.The control strategy can be seen in Figure 7.

$P_{OUT} > P_{PV}$	
PVRR $>$ 0	PVRR $\leq$ 0
$\text{MARR}_{\text{des}} = 0$	$\text{MARR}_{\text{des}} = 0$
$dP_{DC}/dt = \lvert\text{PVRR}\rvert$	$dP_{DC}/dt = {}^{*}RR_{adj}$
$P_{OUT} < P_{PV}$	
PVRR $>$ 0	PVRR $\leq$ 0
$\text{MARR}_{\text{des}} = 0$	$\text{MARR}_{\text{des}} = 0$
$dP_{DC}/dt = {}^{*}RR_{adj}$	$dP_{DC}/dt = \lvert\text{PVRR}\rvert$

Table 3: Constant selection for RR_{COMP} calculation

$^{*}\text{RR}_{\text{adj}}$ is the ramp-rate at which adjustments to the PV output occurs in order to mitigate the fluctuating output. A high RR_{adj} leads to a quicker tracking of the PV output with less fluctuation mitigation while a smaller value will track the output more slowly but with better system output smoothing.

6.1. Fluctuation Mitigation Results

A year of one minute time series irradiance data, from the Sonbesie weather station in Stellenbosch [14], is used to generate PV yield profiles. These profiles are used as inputs to the smoothing model. Various profiles are generated by the ramp-rate model to fit each battery system according to its size. The high and low ramp-rate is tested. This examines the effect that the ramp-rate has on the battery performance. Scaling of the system and its constants are done in order to make the results relevant to PV systems of different sizes. The battery systems are scaled from the PV system to six various sizes, ranging from ten to one hundred percent. 100 % represents the maximum power and energy produced during a clear sunny day. The ramp-rate model was allowed to use the full DoD of the battery system while limiting the ramp-rate. The RR_{lim} is set to 1 %of the maximum PV output. This allows for small amounts of fluctuations which are caused by very light cloud cover or other weather related events. The low ramp-rate is chosen at 20 % of the RR_{lim}. This is just above the ramp-rate at which the P_{PV} increases on a clear-skied, sunny day. The high ramp-rate was chosen at 90 % of the RR_{lim}. This is just below the set ramp-rate

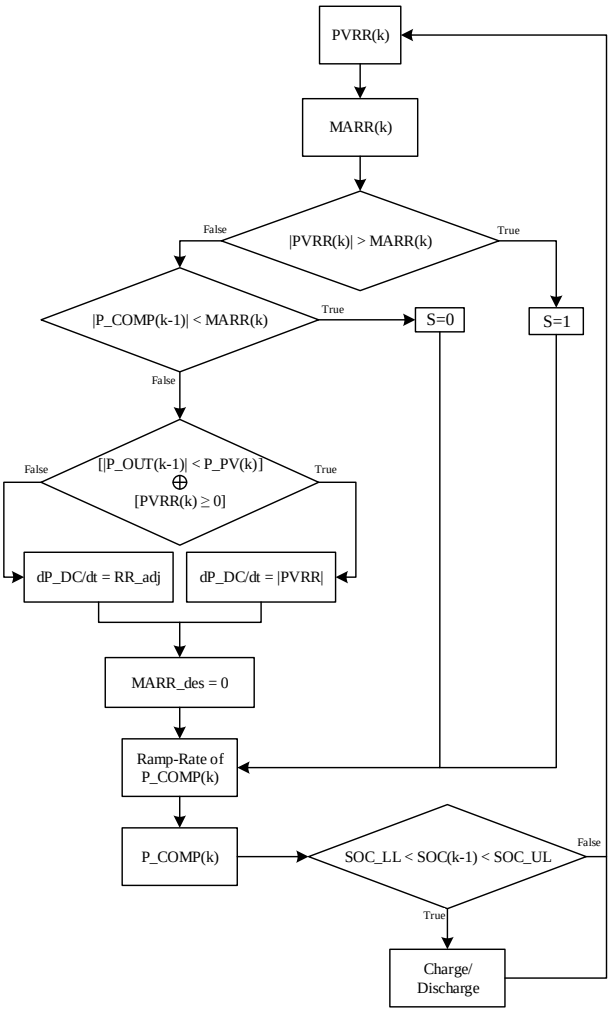

Fig. 7. Ramp-rate control strategy

limit and allows for fluctuations far above the clear-sky fluctuations. The high ramp-rate is chosen at this value to show how the system can monitor for ramp-rates above the limit but still adjust the output to another value just below the limit. The set constants of the model are shown in Table 4.

An example of the fluctuation mitigation can be seen in Figure 8. This example consists of the minute time series weather data of a single day with passing cloud cover. Whenever the ramp-rate exceeds the limit, a near horizontal step is made in the output. This is the model smoothing a sudden drop or rise in the PV output. Once the ramping event passes, the model adjusts the battery output such that the PV output can be tracked again but not exceed the ramp-rate limits while doing so.

The results indicate the SOH of the battery as a percentage of its original capacity and it is clear that Li-ion technology can handle much more Ah-throughput and that a much larger lead-acid battery system is required to compete with the Li-ion technology. At 10 % battery size, the lead acid

Parameters	Value
SOC_{max}	100 %
DoD_{max}	100 %
RR_{lim} (% of max P_{PV})	1 %
High RR_{adj} (% of RR_{lim})	90 %
Low RR_{adj} (% of RR_{lim})	20 %
η_{inv}	89.5 %

Table 4: Ramp-rate model constants

technology's SOH dropped nearly 70 % while the Li-ion lost a little over 4 %. The Li-ion performed about sixteen times better, which is more than the expected ten times. The results of the estimated battery life, based on these specific Ah-throughput profiles, can be examined in Figure 9.

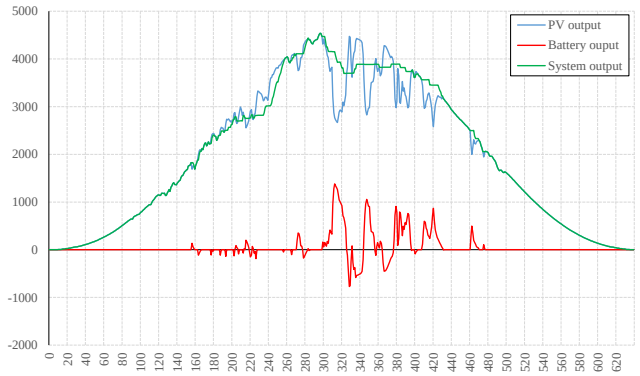

Fig. 8. Example result of actual ramp-rate model

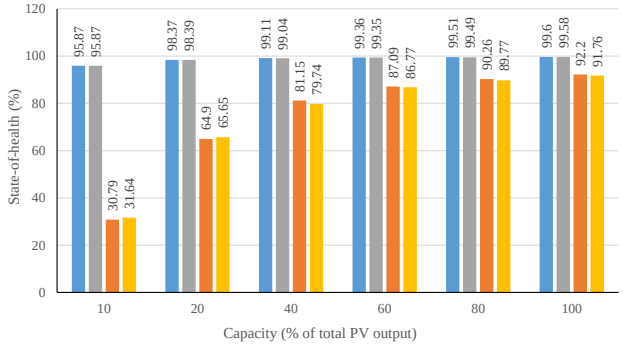

Fig. 9. Battery SOH for different system sizes at different ramp-rates.

7. Conclusion

A battery SOH model was selected and simulations were done using a Li-ion and a lead-acid battery model. The results were compared to physical test results from literature and were found to be similar. Based on this, the SOH model used is found credible. The ramp-rate approach was chosen as a smoothing model. This model served to produce Ah-throughput profiles based on local weather data, for the SOH model. This produced SOH results with which the two battery technologies could be compared for this scenario. The results showed that the lithium-ion ($LiFePO_4$) battery technology experienced the least amount of health loss, owing to its ability to manage much greater energy-throughputs.

The SOH model uses different variations of the Arrhenius equation for the Li-ion and lead-acid batteries. This limits the lead-acid battery from showing the effect the C-rate would have on its SOH results. This raises some concerns when comparing the two battery technologies since this could narrow the gap between the SOH results. The validity of the results can also be questioned with regard to the fluctuation smoothing method because different PV systems do not use the same methods. The researcher wants to suggest a method which could provide the necessary fluctuation smoothing.

Figure 9 assists the reader by informing on the performance of the various battery technologies based on a certain energy-throughput profile. The reader can thus make a price versus performance decision based on the available budget and required lifetime for a certain implementation.

References

[1] W. Howard, C. Schmidt, and E. Scott, "Lithium-ion battery," Jul. 21 2009, US Patent 7,563,541. [Online]. Available: http://www.google.com/patents/US7563541

[2] S. Vazquez, S. M. Lukic, E. Galvan, L. G. Franquelo, and J. M. Carrasco, "Energy Storage Systems for Transport and Grid Applications," *IEEE Transactions on Industrial Electronics*, vol. 57, no. 12, pp. 3881–3895, 2010.

[3] Meridian International Research, "The Trouble with Lithium 2 Under the Microscope," *Meridian International Research*, no. May, pp. 1–54, 2008.

[4] I. Rde and B. A. Andersson, "Requirement for metals of electric vehicle batteries," *Journal of Power Sources*, vol. 93, no. 12, pp. 55 – 71, 2001.

[5] M. Jongerden and B. Haverkort, "Battery modeling," 2008.

[6] M. Chen and G. A. Rincon-Mora, "Accurate electrical battery model capable of predicting runtime and i-v performance," *IEEE Transactions on Energy Conversion*, vol. 21, no. 2, pp. 504–511, June 2006.

[7] H. Bindner, T. Cronin, P. Lundsager, J. Manwell, U. Abdulwahid, and I. Baring-Gould, *Lifetime modelling of lead acid batteries*, 2005.

[8] S. Ebbesen, P. Elbert, and L. Guzzella, "Battery State-of-Health Perceptive Energy Management for Hybrid Electric Vehicles," *IEEE Trans. Veh. Technol.*, vol. 61, no. 7, pp. 2893–2900, 2012.

[9] I. Bloom, B. W. Cole, J. J. Sohn, S. A. Jones, E. G. Polzin, V. S. Battaglia, G. L. Henriksen, C. Motloch, R. Richardson, T. Unkelhaeuser, D. Ingersoll, and H. L. Case, "An accelerated calendar and cycle life study of Li-ion cells," *Journal of Power Sources*, vol. 101, no. 2, pp. 238–247, 2001.

[10] J. Wang, P. Liu, J. Hicks-Garner, E. Sherman, S. Soukiazian, M. Verbrugge, H. Tataria, J. Musser, and P. Finamore, "Cycle-life model for graphite-LiFePO4 cells," *Journal of Power Sources*, vol. 196, no. 8, pp. 3942–3948, 2011.

[11] R. K. Jaworski, "Effects of nonlinearity of Arrhenius equation on predictions of time to failure for batteries exposed to fluctuating temperatures," *Telecommunications Energy Conference, 1998. INTELEC. Twentieth International*, pp. 289–296, 1998.

[12] M. J. E. Alam, K. M. Muttaqi, and D. Sutanto, "A novel approach for ramp-rate control of solar pv using energy storage to mitigate output fluctuations caused by cloud passing," *IEEE Transactions on Energy Conversion*, vol. 29, no. 2, pp. 507–518, June 2014.

[13] W. Marada, "Capacity degradation of lead-acid batteries under variable-depth cycling operation in photovoltaic system," in *Mixed Design of Integrated Circuits Systems (MIXDES), 2015 22nd International Conference*, June 2015, pp. 552–555.

[14] Stellenbosch University, "Stellenbosch Weather, Sonbesie," 2016. [Online]. Available: http://weather.sun.ac.za/

View publication stats